Neutral atom emission in the direction of the high-latitude magnetopause for northward IMF: Simultaneous observations from IMAGE spacecraft and SuperDARN radar

S. Taguchi,[1] K. Hosokawa,[1] A. Nakao,[1] M. R. Collier,[2] T. E. Moore,[2] A. Yamazaki,[3] N. Sato,[4] and A. S. Yukimatu[4]

[1] During a northward interplanetary magnetic field on 27 March 2001, the Low Energy Neutral Atom (LENA) imager on the Imager for Magnetopause-to-Aurora Global Exploration (IMAGE) spacecraft in the magnetosphere observed an enhanced emission in the direction of the very high-latitude magnetopause. Simultaneous observations from IMAGE/LENA and SuperDARN radar show that the LENA emission appears concurrently with the enhancement of the sunward flow of the reverse convection in the ionosphere. The field line mapping from the magnetosphere to the ionosphere suggests that the source ions for the LENA emission are in the sunward flow region. Although the direction of the emission is relatively stable, its direction changes slightly so that the emission may shift poleward or equatorward. From these observations, we suggest that LENA can monitor the ion entry caused by cusp reconnection and that the reconnection site moves on a timescale of several minutes. **Citation:** Taguchi, S., K. Hosokawa, A. Nakao, M. R. Collier, T. E. Moore, A. Yamazaki, N. Sato, and A. S. Yukimatu (2006), Neutral atom emission in the direction of the high-latitude magnetopause for northward IMF: Simultaneous observations from IMAGE spacecraft and SuperDARN radar, *Geophys. Res. Lett.*, *33*, L03101, doi:10.1029/2005GL025020.

1. Introduction

[2] When the interplanetary magnetic field (IMF) is northward, reconnection occurs poleward of the cusp. This cusp reconnection drives reverse convection, which consists of sunward flow in the dayside polar cap and return flow at lower latitudes. The reconnection also causes magnetosheath ions to enter such a sunward convection region. In this region, ions with higher energies appear at high latitudes, and lower energy ions arrive at somewhat lower latitudes, demonstrating reversed ion dispersion. The speed of the fast ion flow at the high-latitude edge has been observed to be 200–400 km s^{-1} by the Polar spacecraft [e.g., *Fuselier et al.*, 2000] or the Cluster spacecraft [e.g., *Phan et al.*, 2003].

[3] It is important to understand the degree to which this fast flow layer exists stably during northward IMF. How-

ever, it is difficult to examine the stability of this phenomenon by in situ spacecraft observations because spacecraft usually reside in that layer for only a few minutes. *Fuselier et al.* [2000] proposed an interesting approach, in which the distance to the reconnection site from the location of the in situ Polar observation is estimated by proton distributions having characteristic low-energy cutoffs. In addition, the stability of the reconnection site for a few tens of minutes has been discussed. However, in order to further our understanding, considering the fact that there are large uncertainties in the method based on the proton distributions from the in situ observation, a remote-sensing approach is required.

[4] In the present study, we show that remote sensing using the Low Energy Neutral Atom (LENA) imager [*Moore et al.*, 2000] on the IMAGE spacecraft can be applied in order to determine the stability of the reconnection site. Several recent studies using LENA have shown that significant source ions, which can produce neutral atom emissions through charge exchange with the Earth's hydrogen exosphere, are present in either the post-shocked flow of the solar wind [*Collier et al.*, 2001a, 2001b], in the magnetosheath flow near the subsolar magnetopause [*Collier et al.*, 2001b; *Moore et al.*, 2003; *Fok et al.*, 2003; *Taguchi et al.*, 2004a; *Collier et al.*, 2005] or the flow in the cusp indentation [*Taguchi et al.*, 2004a, 2004b], as well as in the outflow from the ionosphere [e.g., *Moore et al.*, 2001]. We herein report an event of simultaneous observations from IMAGE/LENA and SuperDARN radar under northward IMF, and show that the ion flow from the cusp reconnection site can be a significant source of LENA emission in the direction of the magnetopause.

2. IMAGE Orbit and Field of View of SuperDARN Radar

[5] At approximately 1600 UT on 27 March 2001, IMAGE was near apogee in the northern hemisphere. We focused on the period for some time after apogee, from 17:30 to 19:40 UT. Figure 1 shows the IMAGE orbit in the X_{GSM}-Z_{GSM} plane for this interval. At 17:30 UT, IMAGE was located near $(X_{GSM}, Z_{GSM}) \sim (2.7\ R_E, 7.4\ R_E)$ in the mid-noon sector ($Y_{GSM} \sim 0\ R_E$).
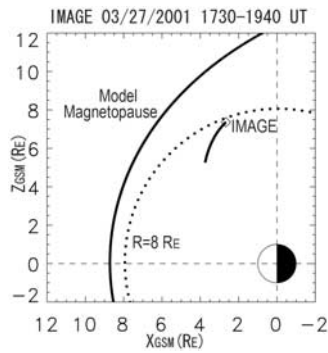
[6] Figure 1 also shows the radial distance of 8 R_E (dotted curve). Inside this radial distance, approximately, the exospheric neutral hydrogen densities increase sharply with the decrease in the geocentric distance, as compared to the density profiles outside this distance [*Østgaard et al.*, 2003]. Since IMAGE is inside this distance, it is expected that the

[1]Department of Information and Communication Engineering, University of Electro-Communications, Tokyo, Japan.
[2]NASA Goddard Space Flight Center, Greenbelt, Maryland, USA.
[3]Graduate School of Science, Tohoku University, Sendai, Japan.
[4]National Institute of Polar Research, Tokyo, Japan.

Figure 1. IMAGE orbit in the X_{GSM}-Z_{GSM} for during the interval of 1730–1940 UT, 27 March 2001. The diamond represents the location of IMAGE at 1730 UT. The dotted curve shows the radial distance of 8 R_E, and the outermost solid curve represents the magnetopause predicted by *Shue et al.* [1998].

neutral atom emission due to charge-exchange of ions with the Earth hydrogen exosphere can be detected from altitudes above and below the spacecraft. The outermost solid curve represents the magnetopause predicted by *Shue et al.* [1998] with the IMF B_Z of 15 nT and a dynamic pressure of 6 nPa, which are representative ACE solar wind conditions for this event.

[7] During the interval of interest, the SuperDARN radar [*Greenwald et al.*, 1995] at Saskatoon, Canada (52.16°N, 106.53°W) monitored plasma convection near the cusp in the ionosphere. The field of view covers the daytime sector from ~09 MLT to ~15 MLT, and significant backscatter signals were obtained from the ionosphere between ~09 MLT and ~13 MLT.

3. Observations

[8] Figure 2 shows variations of ACE solar wind, IMAGE/LENA hydrogen count rate, and line of sight (LOS) velocity obtained using the SuperDARN radar. Figures 2a–2d display the solar wind parameters, which are shifted by 32 min, by relating the ACE detection of an interplanetary shock at 1725 UT with a sudden commencement observed at 1757 UT in the H-component of the SYM index (SYM-H) (Figure 2e). Note that the solar wind convection time ~32 min is not constant. The convection time gets several minutes longer at the end of the interval, as is estimated from the comparison between the southward turning of IMF (Figure 2c) and the change of the ionospheric convection, which is shown later. Figure 2f shows the LENA background-corrected hydrogen data in spectrogram format. The zero degree position in the Y-axis represents the direction of the center of the LENA spin angle sector that is the closest to the solar direction for this interval. We refer to the angle on the Y-axis as solar spin phase (SSP). Figure 2g shows the LOS (poleward) velocity for beam 5 of the SuperDARN Saskatoon radar in the format in which the range gate of the beam is on the Y-axis. Velocity profiles for the three range gates are shown in Figure 2h.

[9] In the LENA data (Figure 2f) the Sun signal [e.g., *Moore et al.*, 2001; *Collier et al.*, 2001a] representing

neutral solar wind is clearly identified as a narrow green line near the zero degree position. In this plot, we consider emissions at angles much greater than the Sun signal. The emission for SSP~90°, which comes primarily from the direction of the very high-latitude magnetopause, is enhanced at 1820 UT.

[10] The sunward flow (green/blue color in Figure 2g) in the ionosphere, which is typical of northward IMF, is enhanced upon the appearance of the LENA emission at 18:20 UT, presumably responding to the increase of the solar wind speed (Figure 2b). Figure 2h shows that the LOS velocity enhancement at this time is roughly 400 ms^{-1}.

[11] From 1820 to 1926 UT, the LENA emission comes primarily from SSP of 90°–150°. Although the direction of the emission is relatively stable, its direction changes
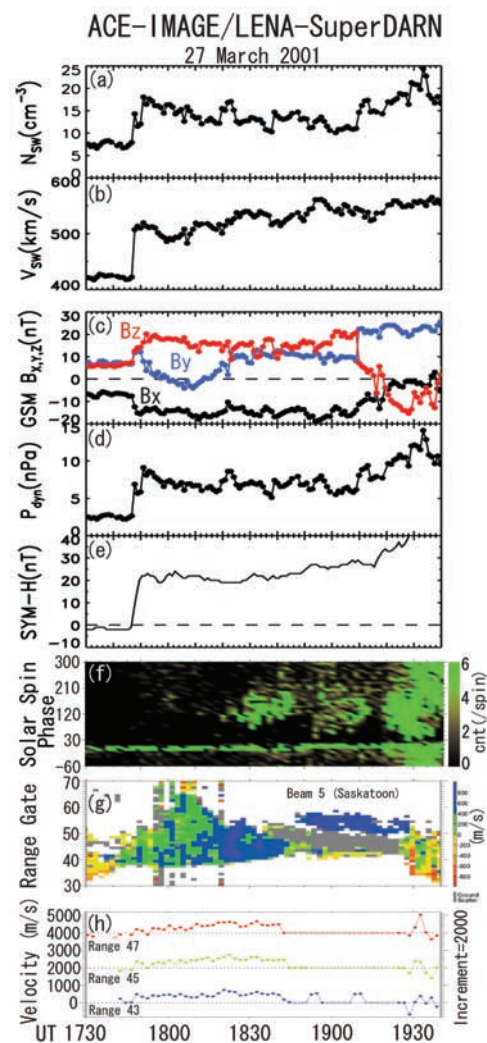
Figure 2. (a) ACE plasma density, (b) velocity, (c) three components of IMF in GSM, (d) dynamic pressure, (e) SYM-H index, (f) LENA spectrogram, (g) line of sight velocity for beam 5 at the SuperDARN Saskatoon radar, and (h) velocity profiles for the range gates 43, 45, 47 of that beam. In Figure 2c, 64-s averages of IMF data that were created from original 16-s averages are plotted so as to make comparison between the IMF and plasma data easier. In Figure 2g gray color simply represents the ground scatter.
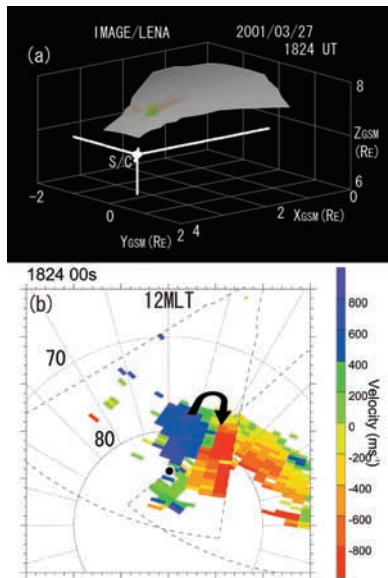
Figure 3. (a) Example of LENA snapshots observed in the direction of the very high latitude magnetopause. Background-corrected hydrogen count rates are plotted on the sphere with a radius of 8 R_E. The location of IMAGE at this time is $(X_{GSM}, Y_{GSM}, Z_{GSM}) \sim (3.2, -0.2, 6.7)$ R_E. (b) Footprint (black dot) of the LENA peak emission on the ionospheric convection map, which is shown in the altitude-adjusted corrected geomagnetic coordinates. The arrow shows the inferred flow pattern.

slightly so that the emission may shift poleward or equatorward. The direction of the emission appears to fluctuate for a while after 1820 UT. Shortly after the emission begins, it spreads over a wider SSP range (from 60° to 200°) around 1830 UT. The SSP then increases during the period from 1832 to 1846 UT. There is no clear variation in SSP for 1848 to 1910 UT. During the period from 1918 to 1926 UT the emission moves to lower angles.

[12] At 1926 UT, the emission distribution drastically changes to cover a much wider angle range than the distribution during 1820–1926 UT. Immediately thereafter, anti-sunward flow appears in the ionosphere (Figure 2g), indicating that the LENA emission no longer exhibits the conditions for northward IMF (Figure 2c) after this time. This suggests that the northward IMF is associated with the emission for 1820–1926 UT.

[13] An example of the LENA snapshots is shown in Figure 3a. In this plot, the hydrogen count rate for each line of sight is plotted on the sphere with a radius of 8 R_E. The peak of the emission can be seen at $(X, Y, Z) = (2.9, -0.1, 7.5)$ R_E. The emission comes from the region somewhat tailward of the spacecraft.

[14] The ionospheric footprint of this position is shown as a black dot on the convection map obtained from the data from SuperDARN radars (Figure 3b). We used the Tsyganenko 96 model with inputs of $(B_Y, B_Z) = (8, 16)$ nT, $P_{dyn} = 8$ nPa, and Dst = 22 nT, although the input of the IMF B_Z (16 nT) for the Tsyganenko 96 model is beyond the range of reliable approximation. In this plot the blue color represents sunward flow having speed of >400 m s^{-1}. The flow is sunward near the local noon and is anti-sunward on

the prenoon side, showing a reverse convection pattern. In addition to the data from Saskatoon, the LOS velocity data from Prince George, which was located in the morning sector at this time, are included. The data from Prince George shows a sunward flow at very high latitudes, i.e. >82°. The black dot can be seen at these high latitudes, suggesting that the source ions for the LENA emission are in the sunward flow region of the reverse convection.

4. Discussion and Conclusions

[15] Figure 4 shows a schematic illustration representing the interpretation of the observations. The dashed gray lines indicate the ion entry caused by reconnection. This fast ion flow produces the neutral atoms through charge exchange with the Earth's hydrogen exosphere if it enters a region of adequate hydrogen density. The bold black lines connecting to the gray lines represent the neutral atom emission produced by the ion entry. IMAGE/LENA can detect the emission when it is located downstream of the ion entry. In other words, a spacecraft residing at a relatively large Z, where LENA can look into the reconnection site roughly along the magnetic field line, would be suitable for monitoring the cusp reconnection. It should be noted that the observed neutral atom image represents an integration of the downgoing magnetosheath ions along that field line.

[16] LENA responds to incident neutrals with energies of from about 10 eV up to 3–4 keV [Moore et al., 2003]. Because of this response, ions with a wide range of speed can be sources for the emission. Magnetosheath ions, having lower speeds, precipitate on the more sunward side because the reconnected field lines (along which the ions enter) move sunward. Hence, the LENA emission due to the cusp reconnection would be observed in a relatively wide spin angle, which is consistent with the observation that the emission occurs at angles of from 90° to 150° (Figure 2). To obtain the exact extension and motion of the reconnection site, further analyses that include the ion dispersion effect quantitatively are needed.

[17] We next perform a rough examination of the possibility that the ion entry produces observable counts of the neutral atom emissions. Assuming that the number density and velocity of the ion entry are ~10 cm^{-3} and ~200 km s^{-1}, respectively, based on a recent Cluster
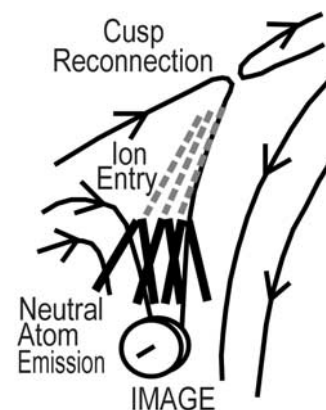
Figure 4. Schematic illustration representing the interpretation of the LENA observations.

observation by *Phan et al.* [2003], the ion flux is $2 \times 10^8 \ \mathrm{cm^{-2}s^{-1}}$. When LENA's field-of-view for a single spin sector falls in the region of the source ion flux, the neutral atom flux, Φ_N, obtained at that spin angle is expressed as the integral of the ion flux, Φ_{ION}, multiplied by the charge exchange cross section, σ, and the hydrogen exospheric density, n_H, along the LOS [e.g., *Collier et al.*, 2001b; *Taguchi et al.*, 2004a].

[18] Although the direction of the dominant LENA emission is not necessarily parallel to the radial direction from the Earth, we assume as a lower limit (from the shortest distance of the LOS integral) that the LOS is in the radial direction from the center of the Earth, and that the charge exchange of the ions is operative between the altitude of IMAGE (at $R \sim 7R_E$) and $R = 10 \ R_E$. In addition, we assume that σ and Φ_{ION} ($= 2 \times 10^8 \ \mathrm{cm^{-2}s^{-1}}$) do not vary along the line of sight from $R = 7 \ R_E$ to $R = 10 \ R_E$. We can calculate the integral of n_H from $R = 7 \ R_E$ to $R = 10 \ R_E$ to be $\sim 5 \times 10^{10} \ \mathrm{cm^{-2}}$ using recent results for the neutral hydrogen density reported by *Østgaard et al.* [2003]. Taking $\sigma \sim 2 \times 10^{-15} \ \mathrm{cm^2}$ [e.g., *Gealy and Van Zyl*, 1987], we obtain $\Phi_N \sim 2 \times 10^4 \ \mathrm{cm^{-2} \ s^{-1}}$.

[19] Taking 5.3×10^{-5} for LENA's neutral hydrogen detection efficiency for the time period of the present observation, a Φ_N of $2 \times 10^4 \ \mathrm{cm^{-2}s^{-1}}$ corresponds to a count rate of $1.1 \ \mathrm{s^{-1}}$ at LENA, the entrance aperture of which has an area of $1 \ \mathrm{cm^2}$. Since each spin sector is observed for approximately 2.7 seconds, this count rate would be approximately 3 count per spin. Thus, the cusp ion entry appears to produce neutral atom emissions that can be detected by LENA. This count is close to the actual 7 count/spin for the peak of the emission (Figure 3a).

[20] This crude estimation also shows that the LENA count can become less than one count level if the ion number flux (Φ_{ION}) decreases from the assumed value by one order. To maintain an adequate ion number flux, the number density of magnetosheath ions must be relatively high, in other words, the solar wind density should be relatively high. In Figure 2, the LENA emissions are weak in a couple of intervals. It appears that these intervals correspond to the relatively low densities ($\sim 10 \ \mathrm{cm^{-3}}$) of the ACE solar wind for 1804–1806 UT (i.e., 1836–1838 UT in Figure 2a) and 1826–1832 UT (i.e., 1858–1904 UT). Hence, the existence of the weak emission does not necessarily indicate that the cusp reconnection pauses. Using proton aurora data from the Far Ultra Violet (FUV) Imager, *Frey et al.* [2003] have shown that the cusp reconnection is continuous, occurring without pause for many hours. No FUV data are available for the interval of the present event.

[21] Our interpretation suggests that a large Z location of IMAGE and a relatively large solar wind density are necessary for monitoring the cusp reconnection as well as a strong northward IMF. From the noon-midnight passes for March to April 2001 we have searched for intervals for ACE solar wind density of $>15 \ \mathrm{cm^{-3}}$, and ACE IMF B_Z of >15 nT, and the IMAGE Z_{GSM} of $>5 \ R_E$. Three intervals have been found including the present event, and similar type of LENA emissions can be seen in those three events.

[22] In conclusion, simultaneous observations from IMAGE/LENA and SuperDARN suggest that LENA can monitor the ion entry caused by cusp reconnection and that the reconnection site moves on a timescale of several minutes.

References

Collier, M. R., et al. (2001a), Observations of neutral atoms from the solar wind, *J. Geophys. Res.*, *106*, 24,893–24,906.

Collier, M. R., et al. (2001b), LENA Observations on March 31, 2001: Magnetosheath Remote Sensing, *Eos. Trans. AGU*, *82*(47), Fall Meeting Suppl., Abstract SM41C-05.

Collier, M. R., T. E. Moore, M.-C. Fok, B. Pilkerton, and S. Boardsen (2005), Low-energy neutral atom signatures of magnetopause motion in response to southward B_z, *J. Geophys. Res.*, *110*, A02102, doi:10.1029/2004JA010626.

Fok, M.-C., et al. (2003), Global ENA IMAGE simulations, *Space Sci. Rev.*, *109*, 77–103.

Frey, H. U., T. D. Phan, S. A. Fuselier, and S. B. Mende (2003), Continuous magnetic reconnection at Earth's magnetopause, *Nature*, *426*, 533–534.

Fuselier, S. A., S. M. Petrinec, and K. J. Trattner (2000), Stability of the high-latitude reconnection site for steady northward IMF, *Geophys. Res. Lett.*, *27*, 473–476.

Gealy, M. W., and B. Van Zyl (1987), Cross sections for electron capture and loss: I. H^+ and H^- impact on H and H_2, *Phys. Rev. A*, *36*, 3091–3099.

Greenwald, R. A., et al. (1995), DARN/SuperDARN: A global view of the dynamics of high-latitude convection, *Space Sci. Rev.*, *71*, 761–796.

Moore, T. E., et al. (2000), The low-energy neutral atom imager for IMAGE, *Space Sci. Rev.*, *91*, 155–195.

Moore, T. E., et al. (2001), Low energy neutral atoms in the magnetosphere, *Geophys. Res. Lett.*, *28*, 1143–1146.

Moore, T. E., et al. (2003), Heliosphere-geosphere interactions using low energy neutral atom imaging, *Space Sci. Rev.*, *109*, 351–371.

Østgaard, N., S. B. Mende, H. U. Frey, G. R. Gladstone, and H. Lauche (2003), Neutral hydrogen density profiles derived from geocoronal imaging, *J. Geophys. Res.*, *108*(A7), 1300, doi:10.1029/2002JA009749.

Phan, T., et al. (2003), Simultaneous Cluster and IMAGE observations of cusp reconnection and auroral proton spot for northward IMF, *Geophys. Res. Lett.*, *30*(10), 1509, doi:10.1029/2003GL016885.

Shue, J.-H., et al. (1998), Magnetopause location under extreme solar wind conditions, *J. Geophys. Res.*, *103*, 17,691–17,700.

Taguchi, S., M. R. Collier, T. E. Moore, M.-C. Fok, and H. J. Singer (2004a), Response of neutral atom emissions in the low- and high-latitude magnetosheath direction to the magnetopause motion under extreme solar wind conditions, *J. Geophys. Res.*, *109*, A04208, doi:10.1029/2003JA010147.

Taguchi, S., K. Hosokawa, M. R. Collier, T. E. Moore, M.-C. Fok, A. S. Yukimatu, N. Sato, and R. A. Greenwald (2004b), Simultaneous observations of the cusp with IMAGE Low Energy Neutral Atom Imager and SuperDARN radar, *Adv. Polar Upper Atmos. Res.*, *18*, 53–64.

————————————
M. R. Collier and T. E. Moore, NASA Goddard Space Flight Center, Greenbelt, MD 20771, USA.

K. Hosokawa, A. Nakao, and S. Taguchi, Department of Information and Communication Engineering, University of Electro-Communications, Chofu, Tokyo, 182-8585, Japan. (taguchi@ice.uec.ac.jp)

N. Sato and A. S. Yukimatu, National Institute of Polar Research, Tokyo, 173-8515, Japan.

A. Yamazaki, Graduate School of Science, Tohoku University, Sendai, 980-8578, Japan.